


Article

# Pubescenosides E–K, Seven New Triterpenoid Saponins from the Roots of *Ilex pubescens* and Their Anti-Inflammatory Activity

Xiaoxu Qiao<sup>1</sup>, Mengying Ji<sup>1</sup>, Yunda Yao<sup>2</sup>, Leilei Ma<sup>1</sup>, Jinjun Wu<sup>1</sup>, Guochao Liao<sup>1</sup>, Hua Zhou<sup>2</sup> , Zhongqiu Liu<sup>1,2</sup> and Peng Wu<sup>1,\*</sup>

- <sup>1</sup> Joint Laboratory for Translational Cancer Research of Chinese Medicine of the Ministry of Education of the People's Republic of China, International Institute for Translational Chinese Medicine, University of Chinese Medicine, Guangzhou 510006, China; qiaoxiaoxu87@126.com (X.Q.); 18826415793@163.com (M.J.); maleilei1@126.com (L.M.); wujinjun@gzucm.edu.cn (J.W.); liaog@zucm.edu.cn (G.L.); liuzq@gzucm.edu.cn (Z.L.)
- <sup>2</sup> State Key Laboratory of Quality Research in Chinese Medicine, Macau University of Science and Technology, Taipa, Macau 999078, China; Yunda\_Yao@126.com (Y.Y.); huazhou2009@gmail.com (H.Z.)
- \* Correspondence: wupeng@gzucm.edu.cn; Tel.: +86-20-3935-8647

Received: 23 May 2018; Accepted: 7 June 2018; Published: 12 June 2018



**Abstract:** Seven new triterpenoid saponins (1–7), together with three known ones (8–10), were isolated from *Ilex pubescens*. Elucidation of their structures was performed based on high-resolution electrospray ionisation mass spectrometry (HR-ESI-MS), infrared spectra (IR), and nuclear magnetic resonance (NMR) spectroscopic data. The anti-inflammatory activity of the isolates toward lipopolysaccharide (LPS)-stimulated RAW264.7 macrophages was investigated. The results demonstrated that compounds 3, 5, and 6 inhibited the expression of inducible nitric oxide synthase (iNOS) protein in comparison with LPS stimulation in RAW264.7 cells.

**Keywords:** *Ilex pubescens*; anti-inflammation; RAW264.7

## 1. Introduction

*Ilex pubescens*, belonging to the plant family Aquifoliaceae, is widely distributed throughout the south of China. The roots and leaves of *Ilex pubescens* have been used in folk medicine for treating thromboangiitis obliterans [1], coronary heart disease [2], and peripheral vascular diseases [3]. The primary components that have been reported from this plant include triterpenoids [4], phenolic glycosides [5], lignan glycosides [6], hemiterpene glycosides [7], and flavonoids [8]. All of the components described above play an important role related to several bioactivities, such as anti-inflammatory [9–12], anticoagulant [13], and antithrombotic activities [14].

Lipopolysaccharide (LPS)-induced macrophages are widely used to study inflammatory responses in vitro [15]. Macrophages are versatile cells that play many roles, and can be activated by external stimuli, such as LPS, to release excessive amounts of inflammatory mediators, including prostaglandin E<sub>2</sub> (PGE<sub>2</sub>), cyclooxygenase-2 (COX-2), and inducible nitric oxide synthase (iNOS) [16,17]. Moreover, iNOS and COX-2 are considered to be the most important inflammatory mediators [16,18]. In our preliminary research, 27 triterpenoid saponins were isolated from *Ilex pubescens*, and some of them showed remarkable anti-inflammatory activity [19]. However, whether other compounds from this plant have anti-inflammatory activity is still unclear. Therefore, we used an LPS-induced macrophage inflammatory model to determine the effect of 10 compounds on the expression levels of iNOS and COX-2 protein.

## 2. Results

### 2.1. Characterization of the Compounds

Pubescenoside **1** (Figure 1) was isolated as a white amorphous powder, and the molecular formula was deduced to be  $C_{47}H_{74}O_{17}$  based on the quasi-molecular ion peak  $[M + COOH]^-$  at  $m/z$  955.4910 (calcd. 955.4908) in the negative-ion HR-ESI-MS (Figure S1, see Supplementary Materials). The sugar component of acid-hydrolyzed **1** gave xylose, glucose, and rhamnose. The glucose and xylose were determined to be D-configuration and the rhamnose be L-configuration, via thin-layer chromatography (TLC) and high-performance liquid chromatography (HPLC) analyses. The IR spectrum demonstrated the presence of hydroxyl ( $3426\text{ cm}^{-1}$ ), alkyl ( $2938\text{ cm}^{-1}$ ), carbonyl ( $1703\text{ cm}^{-1}$ ), and double bond ( $1644\text{ cm}^{-1}$ ) groups. The  $^1\text{H}$  NMR and  $^{13}\text{C}$  NMR (Tables 1 and 2) showed 17 carbon signals for three sugar moieties and 30 carbons for the aglycone, including one ketone group at  $\delta_C$  212.0 (C-19); one di-substituted double bond ( $\delta_H$  5.62,  $\delta_C$  127.7, C-11;  $\delta_H$  6.16,  $\delta_C$  130.8, C-12); one tri-substituted double bond ( $\delta_C$  142.5, C-13;  $\delta_H$  5.88,  $\delta_C$  129.6, C-18); one carboxyl ( $\delta_C$  178.9, COOR-28); six singlets for tertiary methyls at  $\delta_H$  0.82, 0.85, 1.06, 1.10, 1.34 and 2.21; one methyl doublet at  $\delta_H$  1.08; and anomeric protons of three sugar units ( $\delta_H$  4.91,  $\delta_C$  106.2;  $\delta_H$  5.79,  $\delta_C$  102.6;  $\delta_H$  6.39,  $\delta_C$  102.3). When compared with 3 $\beta$ -hydroxy-19-oxo-18,19-seco-11,13(18)-ursa-diene-28-oic acid [20], their structures were very similar, except for the additional sugar units at C-3 in **1**. The heteronuclear multiple bond correlation (HMBC) analysis results were as follows: from H-3 to C-4, C-23, C-24, and inner-Xyl-C-1; from H-12 to C-9, C-11, C-13, and C-14; from H-18 to C-14, C-16, C-17, and C-22; and from CH<sub>3</sub>-30 to C-19, C-20, and C-21. The HMBC from terminal-Rha-H-1 ( $\delta_H$  6.39, s) to the intermediate-Glc-C-2 ( $\delta_C$  79.7), and from the intermediate-Glc-H-1 ( $\delta_H$  5.79, d,  $J = 5.8$  Hz) to the inner-Xyl-C-2 ( $\delta_C$  79.3), established the linkages of the sugar moieties (Figure 2). The rotating frame overhauser effect spectroscopy (ROESY) correlations of H-3/H-5, H-5/H-9, and H-9/Me-27 revealed Me-27 to be  $\alpha$ -oriented, and the correlations of Me-23/Me-25 and Me-25/Me-26 indicated that the sugar moieties of C-3, Me-23, Me-25, and Me-26 were determined to be in  $\beta$ -orientations (Figure 3). Along with further analyses of the  $^1\text{H}$ - $^1\text{H}$  correlation spectroscopy ( $^1\text{H}$ - $^1\text{H}$  COSY), heteronuclear single quantum coherence (HSQC), and HMBC spectra, compound **1** was finally identified as 3 $\beta$ -[ $\alpha$ -L-rhamnopyranosyl-(1 $\rightarrow$ 2)- $\beta$ -D-glucopyranosyl-(1 $\rightarrow$ 2)- $\beta$ -D-xylopyranosyl]-urs-19-oxo-18,19-seco-11,13(18)-dien-28-oic acid (Figure 1).

The molecular formula of Pubescenoside **2** (Figure 1), a white amorphous powder, was determined to be  $C_{53}H_{84}O_{22}$  by the HRESIMS ion at  $m/z$  1071.5388  $[M - H]^-$  (calcd. 1071.5381) and NMR data. The IR spectrum revealed the existence of hydroxyl, olefinic, and carboxyl absorption bands. The sugar components of acid-hydrolyzed **2** included D-Xylose, D-glucoses, and L-rhamnose, as identified by TLC and HPLC analyses. The  $^{13}\text{C}$  NMR spectrum (Table 2) showed 53 carbon signals, including 23 carbon signals belonging to the sugar units and 30 carbon signals belonging to the aglycone part. It also revealed one ketone group at  $\delta_C$  212.3 (C-19), one carboxyl at  $\delta_C$  175.1 (C-28), and four anomeric carbons. The  $^1\text{H}$  NMR spectrum (Table 1) of **2** displayed signals assignable to six angular methyl groups at  $\delta_H$  0.76, 0.82, 1.03 (6H), 1.32, and 2.13 and one methyl doublet at  $\delta_H$  1.04. The structure of **2** resembled that of **1**, except for an additional glucose unit at C-28. The HMBC from Glc-H-1 to C-28 and inner-Xyl-H-1 to C-3 demonstrated glycosylation sites at the 28-O- and 3-O- positions. Eventually, compound **2** was elucidated as  $\beta$ -D-glucopyranosyl 3 $\beta$ -[ $\alpha$ -L-rhamnopyranosyl-(1 $\rightarrow$ 2)- $\beta$ -D-glucopyranosyl-(1 $\rightarrow$ 2)- $\beta$ -D-xylopyranosyl]-urs-19-oxo-18,19-seco-11,13(18)-dien-28-oate (Figure 1).

The HR-ESI-MS of Pubescenoside **3** (Figure 1) displayed a molecular ion peak  $[M + COOH]^-$  at  $m/z$  1103.5642 (calcd. 1103.5644), indicating that its molecular formula was  $C_{53}H_{86}O_{21}$ . The IR data also manifested absorption bands for hydroxyl, alkyl, carbonyl, and double bond groups. The  $^1\text{H}$  NMR and  $^{13}\text{C}$  NMR data (Tables 1 and 2) of compound **3** demonstrated 23 carbon signals for sugar moieties and 30 carbons for the aglycone, including one tri-substituted double bond ( $\delta_H$  5.41,  $\delta_C$  123.1, C-12;  $\delta_C$  144.4, C-13), one ester carbonyl carbon at C-28 ( $\delta_C$  176.8), four anomeric carbon

signals, and seven methyl singlets at  $\delta_H$  0.82, 0.87, 0.91, 1.07 (6H), 1.24, and 1.33. The NMR data of **3** and 3- $\beta$ -O-[[O- $\beta$ -D-galactopyranosyl-(1 $\rightarrow$ 3)- $\beta$ -D-glucopyranosyl-(1 $\rightarrow$ 2)]- $\beta$ -D-glucopyranosyl]oleanolic acid 28- $\beta$ -D-glucopyranosyl ester [21] were highly similar, with the main difference being the type and connection of the sugar at C-3. The HMBC analysis results were as follows: from H-12 to C-9 and C-14; from H-24 to C-3, C-4, and C-5; from H-27 to C-13, C-14, and C-15; from H-29 to C-19, C-20, and C-21; from inner-Xyl-H-1 to C-3; and from the intermediate-Glc-H-1 to the inner-Xyl-C-2. When combined with comprehensive analyses of  $^1H$ - $^1H$  COSY, HMBC, HSQC, and NOESY NMR spectra, we identified the structure of compound **3** to be  $\beta$ -D-glucopyranosyl 3 $\beta$ -[ $\alpha$ -L-rhamnopyranosyl-(1 $\rightarrow$ 2)- $\beta$ -D-glucopyranosyl-(1 $\rightarrow$ 2)- $\beta$ -D-xylopyranosyl]-olean-12-en-28-oate (Figure 1).

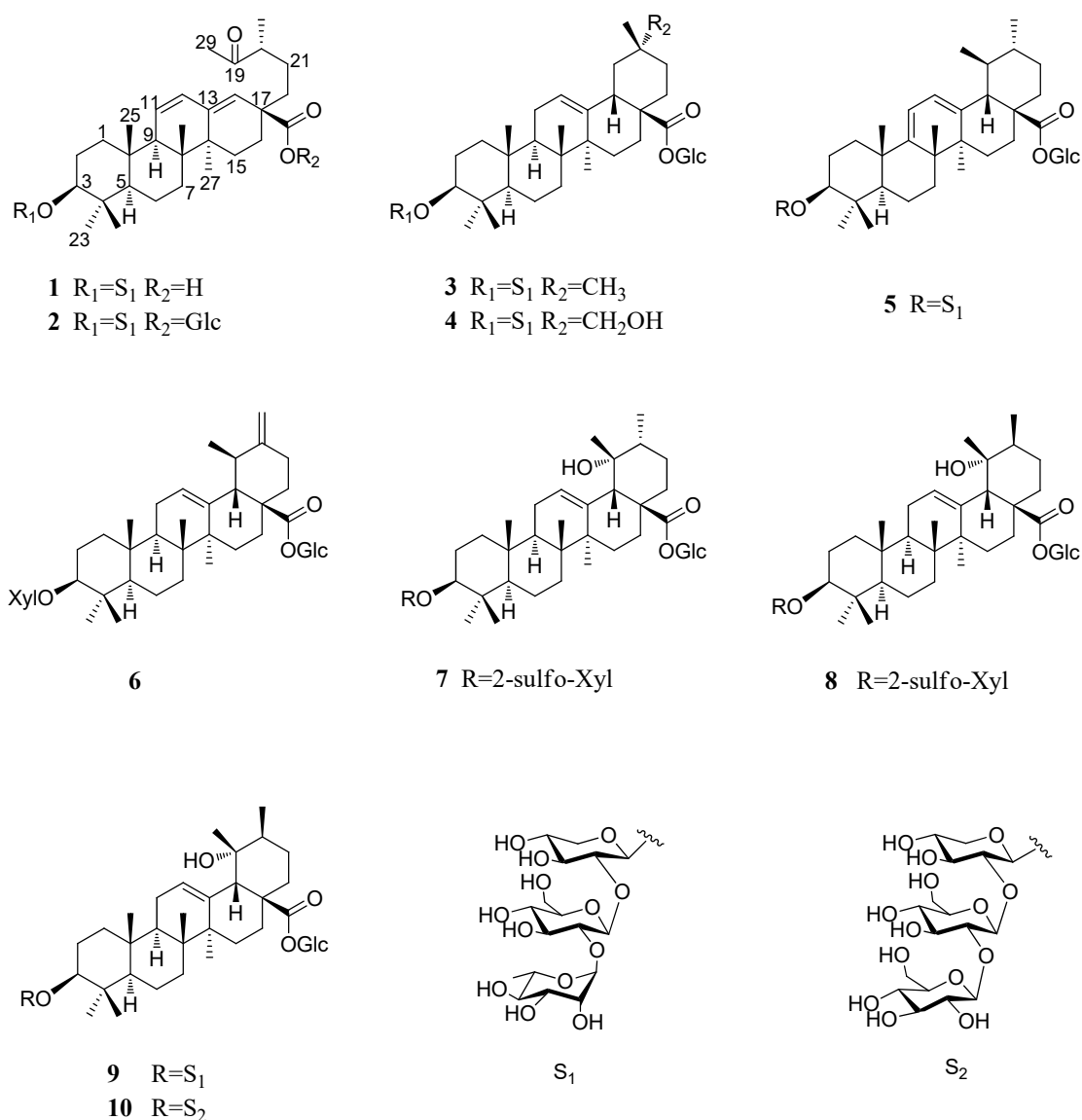


Figure 1. Structures of compounds 1–10.

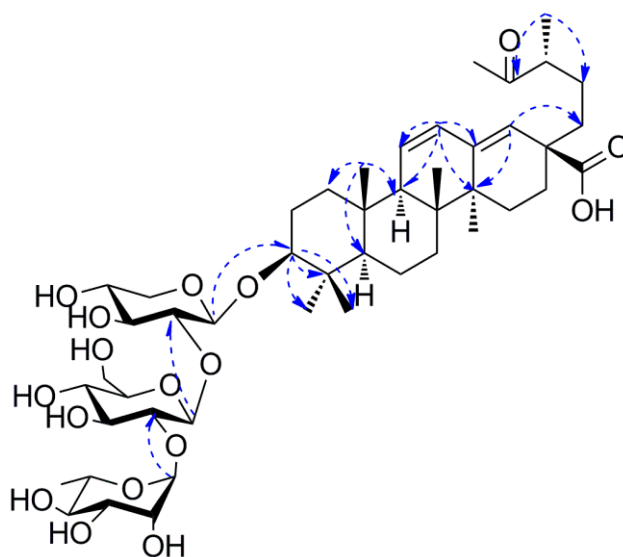


Figure 2. Key HMBC correlations of compound 1.

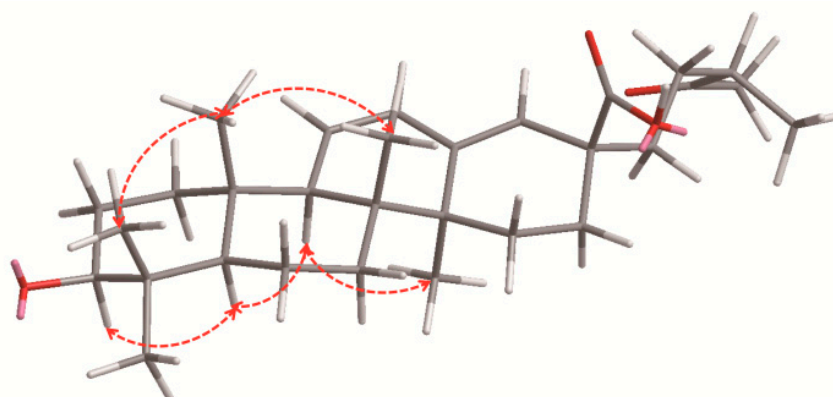


Figure 3. Key ROESY correlations of compound 1.

The HR-ESI-MS data ( $[M - H]^-$  at  $m/z$  1073.5614, calcd. 1073.5538) indicated that the molecular formula of Pubescenoside H (4) was  $C_{53}H_{86}O_{22}$ . The IR spectrum demonstrated the existence of hydroxyl, olefinic, and carboxyl absorption bands. The configurations of the sugar units were determined by hydrolysis to be D-Xylose, D-glucoses, and L-rhamnose. The  $^1H$  NMR and  $^{13}C$  NMR spectrum (Tables 1 and 2) gave six methyl proton signals at  $\delta_H$  0.83, 1.08 (6H), 1.09, 1.25, and 1.32; one double bond ( $\delta_H$  5.45,  $\delta_C$  123.1, C-12;  $\delta_C$  144.6, C-13); one quaternary carbon at C-29 ( $\delta_C$  74.0); one ester carbonyl carbon at C-28 ( $\delta_C$  176.8); and anomeric protons of the four sugar units (3-O-inner-Xyl-1,  $\delta_H$  4.88,  $\delta_C$  106.1; intermediate-Glc-1,  $\delta_H$  5.82,  $\delta_C$  102.5; terminal-Rha-1,  $\delta_H$  6.40,  $\delta_C$  102.3; 28-O-Glc-1,  $\delta_H$  6.33,  $\delta_C$  96.0). The NMR data for compound 4 were almost same as for compound 3, except for the additional hydroxyl group at C-29. The linkages were confirmed by observation of HMBC from H-29 ( $\delta_H$  3.56) to C-19 ( $\delta_C$  41.2), C-20 ( $\delta_C$  36.7), and C-21 ( $\delta_C$  29.1). Based on these results, the structure of 4 was established as  $\beta$ -D-glucopyranosyl 3 $\beta$ -[ $\alpha$ -L-rhamnopyranosyl-(1 $\rightarrow$ 2)- $\beta$ -D-glucopyranosyl-(1 $\rightarrow$ 2)- $\beta$ -D-xylopyranosyl]-29 $\alpha$ -hydroxyursolean-12-en-28-oate (Figure 1).

Pubescenoside I (5) was obtained as a white amorphous powder with the molecular formula  $C_{53}H_{84}O_{21}$  (HR-ESI-MS:  $m/z$  1101.5488  $[M + COOH]^-$ ). In the IR spectrum, absorption bands for hydroxyl ( $3396\text{ cm}^{-1}$ ), alkyl ( $2930\text{ cm}^{-1}$ ), carbonyl ( $1729\text{ cm}^{-1}$ ), and double bond groups ( $1641\text{ cm}^{-1}$ ) were observed. The configuration of the sugar units was ascertained by hydrolysis to

be D-Xylose, D-glucoses, and L-rhamnose. The  $^{13}\text{C}$  NMR data (Table 2) indicated that compound **5** had 53 carbon signals, containing 30 carbon signals in the aglycone and 23 carbon signals in the sugar unit. The 1D and 2D NMR spectra (Tables 1 and 2) revealed the presence of one tri-substituted double bond ( $\delta_{\text{C}}$  134.6, C-9;  $\delta_{\text{H}}$  6.58,  $\delta_{\text{C}}$  128.6, C-11); another tri-substituted double bond ( $\delta_{\text{H}}$  5.61,  $\delta_{\text{C}}$  125.8, C-12;  $\delta_{\text{C}}$  138.6, C-13); one ester carbonyl carbon at C-28 ( $\delta_{\text{C}}$  176.5); four anomeric signals ( $\delta_{\text{H}}$  4.84,  $\delta_{\text{C}}$  106.1;  $\delta_{\text{H}}$  5.71,  $\delta_{\text{C}}$  102.2;  $\delta_{\text{H}}$  6.30,  $\delta_{\text{C}}$  102.1;  $\delta_{\text{H}}$  6.23,  $\delta_{\text{C}}$  96.2); five tertiary methyl at  $\delta_{\text{H}}$  0.81, 0.98, 0.99, 1.04, and 1.27 and two methyl doublets at  $\delta_{\text{H}}$  1.32 (d,  $J = 7.0$  Hz) and  $\delta_{\text{H}}$  0.76 (d,  $J = 5.9$  Hz). The results described above indicated that Pubescenoside **I** (**5**) was highly similar to ilexsaponin **L** [19], except for an additional sugar unit. The HMBC correlations from terminal-Rha-H-1 ( $\delta_{\text{H}}$  6.30, s) to the intermediate-Glc-C-2 ( $\delta_{\text{C}}$  79.5) and from the intermediate-Glc-H-1 ( $\delta_{\text{H}}$  5.71, d,  $J = 6.8$  Hz) to the inner-Xyl-C-2 ( $\delta_{\text{C}}$  79.0), established the linkages of the sugar moieties. Finally, we identified the structure as  $\beta$ -D-glucopyranosyl 3 $\beta$ -[ $\alpha$ -L-rhamnopyranosyl-(1 $\rightarrow$ 2)- $\beta$ -D-glucopyranosyl-(1 $\rightarrow$ 2)- $\beta$ -D-xylopyranosyl]-urs-9(11),12-dien-28-oate (Figure 1).

Pubescenoside **J** (**6**) was obtained as white amorphous powder and had a molecular formula of  $\text{C}_{41}\text{H}_{64}\text{O}_{12}$ , deduced from an ion peak in the HR-ESI-MS at  $m/z$  793.4462 [ $\text{M} + \text{COOH}$ ] $^{-}$  (calcd. for  $\text{C}_{42}\text{H}_{64}\text{O}_{14}^{-}$ , 793.4380). The IR spectrum of **6** showed hydroxyl, alkyl, and carbonyl moieties at  $3385\text{ cm}^{-1}$ ,  $2941\text{ cm}^{-1}$ , and  $1729\text{ cm}^{-1}$ , respectively. The sugar components of acid-hydrolyzed **6** included D-xylose and D-glucose, as identified through TLC and HPLC analyses. The  $^1\text{H}$  NMR and  $^{13}\text{C}$  NMR spectrum (Tables 1 and 2) of the aglycone of **6** revealed five singlets for tertiary methyls at  $\delta_{\text{H}}$  0.88, 0.99, 1.09, 1.27, and 1.31; one methyl doublet at  $\delta_{\text{H}}$  1.06 (d,  $J = 7.1$  Hz); one carboxylic acid ( $\delta_{\text{C}}$  176.5, COOH-28); and two anomeric signals ( $\delta_{\text{H}}$  4.86,  $\delta_{\text{C}}$  108.0, CH-Xyl-1;  $\delta_{\text{H}}$  6.34,  $\delta_{\text{C}}$  96.3, CH-Glc-1). The HMBC analysis was as follows: from H-12 to C-9, C-11 and C-14; from H-18 to C-12, C-13, C-14, C-16, C-17, C-20, C-28 and C-30; from H-25 to C-1, C-5, and C-9; and from H-30 to C-18, C-19 and C-20. A precise comparison of its  $^1\text{H}$  and  $^{13}\text{C}$  NMR data with those of ilexsaponin **I** [19] indicated structural similarity, except for an additional sugar unit in ilexsaponin **I**. Finally, **6** was elucidated as  $\beta$ -D-glucopyranosyl 3 $\beta$ - $\beta$ -D-xylopyranosyl-urs-12,20(30)-dien-28-oate (Figure 1).

The molecular formula of Pubescenoside **K** (**7**) was inferred from the HR-ESI-MS(negative ion mode) result, which displayed [ $\text{M} - \text{H}$ ] $^{-}$  ions at  $m/z$  845.4052 (calcd. for  $\text{C}_{41}\text{H}_{66}\text{O}_{16}\text{S}-\text{H} = 845.3999$ ). The IR spectrum also showed absorption signals for hydroxyl, double bond, and ester groups. The  $^1\text{H}$  NMR data (Table 1) of **7** showed six singlets for tertiary methyls at  $\delta_{\text{H}}$  0.89, 1.14, 1.18, 1.42 (6H), and 1.73, and one methyl doublet at  $\delta_{\text{H}}$  1.11. Furthermore, signals for one tri-substituted double bond ( $\delta_{\text{H}}$  5.57,  $\delta_{\text{C}}$  128.4, C-12;  $\delta_{\text{C}}$  139.3, C-13), one ester carbonyl carbon at C-28 ( $\delta_{\text{C}}$  177.3), one xylopyranose linked to C-3 of the aglycone, and one  $\beta$ -D-glucopyranose linked to C-28 of the aglycone were observed. The HMBC analysis results were as follows: from H-12 to C-9, C-14, and C-18; from H-18 to C-16, C-17, C-19, and C-20; from H-23 to C-3, C-4 and C-5; from H-25 to C-1, C-5, C-9 and C-10; from H-30 to C-19, C-20, and C-21; and from inner-Xyl-H-1 to C-3. The difference between compound **7** and ilexpublesnin **E** [4] was that compound **7** had sulfonylation on the hydroxyl attached to Xyl-C-2, whereas ilexpublesnin **E** is connected to three sugar units at C-3. Therefore, based on the above analysis, compound **7** was deduced as  $\beta$ -D-glucopyranosyl 3 $\beta$ -[(2-O-sulfo- $\beta$ -D-xylopyranosyl)oxy]-19 $\alpha$ -hydroxy-urs-12-en-28-oate (Figure 1).

Additionally, three known compounds (**8–10**) (Figure 1) were also isolated, and their structures were identified as ilexpublesnin **I** (**8**) [4], ilexoside **O** (**9**) [2], and ilexpublesnin **J** (**10**) [4], by comparison of their  $^1\text{H}$  and  $^{13}\text{C}$  NMR, as well as MS data with reported values.

**Table 1.** <sup>1</sup>H NMR spectroscopic data of compounds 1–7 (in pyridine-*d*<sub>5</sub>).

Position	1 <sup>a</sup>	2 <sup>b</sup>	3 <sup>b</sup>	4 <sup>b</sup>	5 <sup>b</sup>	6 <sup>b</sup>	7 <sup>b</sup>
1	0.95 m; 1.77 m	0.94 m; 1.71 m	0.95 m; 1.50 m	0.91 m; 1.46 m	0.97 m; 1.75 m	0.98 m; 1.48 m	0.90 m; 1.54 m
2	1.68 m; 2.56 m	1.75 m; 2.12 m	1.88 m; 2.06 m	1.86 m; 2.09 m	1.96 m; 2.13 m	1.89 m; 2.17 m	1.93 m; 2.12 m
3	3.30 dd (11.6, 3.7)	3.28 dd (11.5, 4.1)	3.28 dd (11.4, 3.6)	3.27 dd (11.4, 4.1)	3.27 dd (10.7, 3.1)	3.40 dd (11.5, 3.8)	3.29 dd (10.8, 2.5)
5	0.83 m	0.79 m	0.80 m	0.76 m	0.76 m	0.81 m	0.80 m
6	1.33 m; 1.54 m	1.27 m; 1.52 m	1.30 m; 1.49 m	1.25 m; 1.44 m	1.26 m; 1.47 m	1.27 m; 1.46 m	1.27 m; 1.45 m
7	1.33 m	1.26 m	1.46 m	1.31 m; 1.43 m	1.16 m	1.37 m; 1.46 m	1.40 m; 1.54 m
9	2.04 m	1.98 m	1.63 m	1.61 m	-	1.76 m	1.78 m
11	5.62 d (10.2)	5.59 d (9.8)	1.93 m	1.87 m	6.58 d (10.1)	1.91 m; 1.98 m	2.0 m; 2.06 m
12	6.18 d (8.5)	6.03 d (10.1)	5.42 s	5.45 s	5.61 d (10.6)	5.48 s	5.57 s
15	1.24 m; 1.92 m	1.16 m; 1.90 m	1.17 m; 2.33 m	1.15 m; 2.32 m	0.88 m; 1.93 m	1.17 m; 2.35 m	1.26 m; 2.44 m
16	1.23 m; 2.15 m	1.30 m; 2.13 m	1.17 m; 1.26 m	1.99 m; 2.16 m	1.64 m; 2.15 m	1.85 m; 1.99 m	3.12 m
18	5.88s	5.72 s	3.19 m	3.28 m	1.92 m	3.99 s	2.92 m
19	-	-	1.25 m; 1.75 m	1.40 m; 2.11 m	2.30 m	2.59 m	-
20	2.53 m	2.50 m	-	-	1.44 m	-	1.36 m
21	1.33 m; 1.66 m	1.32 m; 1.59 m	1.08 m; 1.33 m	1.24 m; 1.74 m	1.50 m; 1.58 m	1.28 m; 1.76 m	2.04 m; 2.12 m
22	1.99 m	1.95 m	1.75 m; 1.97 m	1.73 m; 1.84 m	1.28 m; 2.62 m	1.76 m; 2.08 m	1.79 m; 2.04 m
23	1.34 s	1.32 s	1.33 s	1.32 s	1.27 s	1.31 s	1.42 s
24	1.06 s	1.03 s	1.07 s	1.08 s	1.04 s	0.99 s	1.18 s
25	0.82 s	0.76 s	0.82 s	0.83 s	0.81 s	0.88 s	0.89 s
26	0.85 s	0.82 s	1.07 s	1.09 s	0.98 s	1.09 s	1.14 s
27	1.06 s	1.03 s	1.24 s	1.25 s	0.99 s	1.27 s	1.73 s
29	2.11 s	2.13 s	0.91 s	3.56 m	1.32 d (4.0)	1.06 d (6.7)	1.42 s
30	1.08 d (8.7)	1.03 d (7.1)	0.87 s	1.08 s	0.76 d (5.9)	5.04 <sup>c</sup>	1.11 d (6.2)
3-O-	Xyl	Xyl	Xyl	Xyl	Xyl	Xyl	2-sulfo-Xyl
1	4.92 d (5.2)	4.89 d (6.7)	4.88 d (6.6)	4.88 d (6.6)	4.84 d (6.1)	4.85 d (7.4)	4.97 d (6.6)
2	4.42 <sup>e</sup>	4.01 <sup>c</sup>	4.29 <sup>d</sup>	4.28 <sup>d</sup>	4.22 <sup>d</sup>	4.03 m	5.05 m
3	3.87 m	3.87 m	3.88 m	3.86 m	3.84 m	4.17 m	4.43 m
4	4.08 <sup>c</sup>	4.06 <sup>c</sup>	4.08 <sup>c</sup>	4.06 <sup>c</sup>	4.02 <sup>c</sup>	4.21 m	4.21 m
5	3.73 m; 4.28 <sup>d</sup>	3.72 m; 4.28 <sup>d</sup>	3.72 m; 4.28 <sup>d</sup>	3.72 m; 4.27 <sup>d</sup>	3.68 m; 4.25 <sup>d</sup>	3.78 m; 4.38 m	3.74 m; 4.21 m
Intermediate	Glc	Glc	Glc	Glc	Glc	Glc	
1	5.79 d (5.8)	5.80 d (7.3)	5.81 d (7.8)	5.82 d (7.2)	5.71 d (6.8)		
2	4.24 <sup>d</sup>	4.27 <sup>d</sup>	4.24 <sup>d</sup>	4.22 <sup>d</sup>	4.22 <sup>d</sup>		
3	4.48 <sup>e</sup>	4.44 <sup>e</sup>	4.44 <sup>c</sup>	4.41 <sup>e</sup>	4.39 <sup>e</sup>		
4	4.07 <sup>c</sup>	4.06 <sup>c</sup>	4.04 <sup>c</sup>	4.03 <sup>c</sup>	3.83 m		

Table 1. Cont.

Position	1 <sup>a</sup>	2 <sup>b</sup>	3 <sup>b</sup>	4 <sup>b</sup>	5 <sup>b</sup>	6 <sup>b</sup>	7 <sup>b</sup>
5	4.28 <sup>d</sup>	4.27 <sup>d</sup>	4.43 <sup>e</sup>	4.29 <sup>d</sup>	4.39 <sup>e</sup>		
6	4.27 <sup>d</sup> ; 4.50 <sup>e</sup>	4.28 <sup>d</sup> ; 4.51 <sup>e</sup>	4.28 <sup>d</sup> ; 4.51 <sup>e</sup>	4.27 <sup>d</sup> ; 4.48 <sup>e</sup>	4.21 <sup>d</sup> ; 4.48 <sup>e</sup>		
Terminal	Rha	Rha	Rha	Rha	Rha		
1	6.39 br s	6.38 br s	6.39 br s	6.40 br s	6.30 br s		
2	4.71 m	4.71 m	4.75 m	4.76 m	4.69 s		
3	4.04 <sup>c</sup>	4.05 <sup>c</sup>	4.04 <sup>c</sup>	4.04 <sup>c</sup>	3.95 <sup>c</sup>		
4	4.33 <sup>d</sup>	4.34 <sup>d</sup>	4.34 <sup>e</sup>	4.23 <sup>d</sup>	4.29 <sup>d</sup>		
5	5.03 m	5.04 m	5.04 m	5.04 m	4.98 m		
6	1.81 <sup>f</sup>	1.78 <sup>f</sup>	1.79 d (6.0)	1.8 d (6.0)	1.75 d (5.5)		
28-O-		Glc	Glc	Glc	Glc	Glc	Glc
1		6.32 d (8.2)	6.32 d (8.4)	6.35 d (7.8)	6.23 d (7.8)	6.34 d (8.1)	6.25 d (7.8)
2		4.48 <sup>e</sup>	4.21 <sup>d</sup>	4.33 <sup>e</sup>	4.13 <sup>d</sup>	4.23 m	4.24 m
3		4.44 <sup>e</sup>	4.29 <sup>d</sup>	4.41 <sup>e</sup>	4.39 <sup>e</sup>	4.04 m	4.33 <sup>c</sup>
4		4.29 <sup>d</sup>	4.35 <sup>e</sup>	4.35 <sup>e</sup>	4.23 <sup>d</sup>	4.37 m	4.33 <sup>c</sup>
5		4.44 <sup>e</sup>	4.29 <sup>d</sup>	4.28 <sup>d</sup>	4.22 <sup>d</sup>	4.30 m	4.08 m
6		4.29 <sup>d</sup>	4.43 <sup>e</sup>	4.39 <sup>e</sup> ; 4.45 <sup>e</sup>	4.27 <sup>d</sup> ; 4.39 <sup>e</sup>	4.38 m; 4.47 m	4.39 m; 4.50 m

$\delta$  in ppm;  $J$  in Hz; <sup>a</sup> NMR spectra recorded at 400 MHz; <sup>b</sup> NMR spectra recorded at 600 MHz; <sup>c-f</sup> overlapped signals, assignments may be interchangeable.

**Table 2.**  $^{13}\text{C}$  NMR spectroscopic data of compounds 1–7 (in pyridine- $d_5$ ).

Position	1 <sup>a</sup>	2 <sup>b</sup>	3 <sup>b</sup>	4 <sup>b</sup>	5 <sup>b</sup>	6 <sup>b</sup>	7 <sup>b</sup>
1	38.6	38.5	39.1	39.1	38.3	39.1	38.8
2	27.9	26.6	26.8	26.8	26.6	27.1	26.5
3	89.9	89.8	89.9	89.9	89.9	89.0	89.7
4	40.1	40.1	40.0	40.0	39.9	39.9	39.6
5	55.7	55.7	56.2	56.2	55.5	56.4	55.8
6	18.6	18.5	18.8	18.8	18.6	18.9	18.6
7	32.8	32.6	32.8	33.4	32.8	33.7	33.4
8	41.1	41.1	40.1	40.2	43.4	40.1	40.5
9	54.8	54.8	48.3	48.3	134.6	48.4	47.6
10	37.0	36.9	37.2	37.3	36.7	37.4	36.9
11	127.7	128.4	24.1	24.1	128.6	24.2	24.0
12	130.8	130.4	123.1	123.1	125.8	127.9	128.4
13	142.5	143.9	144.4	144.6	138.6	137.7	139.3
14	41.8	41.7	42.4	42.4	41.6	43.1	42.0
15	26.8	26.7	28.5	28.6	25.4	28.7	29.2
16	27.0	27.9	23.7	23.7	33.4	26.6	26.0
17	48.0	48.0	47.3	47.7	51.8	49.6	48.6
18	129.6	127.0	42.0	41.5	55.4	47.5	54.4
19	212	212.3	46.5	41.2	45.0	37.6	72.6
20	47.8	47.6	31.0	36.7	39.7	153.6	42.1
21	28.5	28.0	34.2	29.1	33.6	28.2	26.6
22	39.3	38.9	33.4	32.3	40.2	31.9	37.7
23	28.4	28.4	28.6	28.6	28.1	28.5	28.3
24	16.5	16.4	17.0	17.0	16.2	17.3	16.9
25	18.3	18.3	15.8	15.8	18.4	16.1	15.6
26	17.1	16.9	17.7	17.8	16.9	17.6	17.3
27	20.4	20.2	26.3	26.3	19.3	26.0	24.6
28	178.9	175.1	176.8	176.8	176.5	176.5	177.3
29	28.2	28.3	33.4	74.0	21.1	21.1	27.0
30	16.6	16.5	23.9	20.0	20.5	113.1	16.7
3-O-	Xyl	Xyl	Xyl	Xyl	Xyl	Xyl	2-sulfo-Xyl
1	106.2	106.2	106.1	106.1	106.1	108	104.8
2	79.3	79.7	79.7	79.7	79.0	75.9	80.2
3	78.1	78.2	78.2	78.2	78.0	79.0	77.2
4	71.6	71.6	71.6	71.6	71.4	71.6	70.7
5	67.0	66.9	66.9	67.0	66.8	67.4	65.9
Intermediate	Glc	Glc	Glc	Glc	Glc		
1	102.6	102.5	102.5	102.5	102.2		
2	79.7	79.6	79.6	79.6	79.5		
3	79.4	79.3	79.4	79.4	79.1		
4	72.7	72.9	72.9	73.0	72.4		
5	78.9	79.0	79.2	79.3	78.7		
6	63.6	63.6	63.6	63.6	63.4		
Terminal	Rha	Rha	Rha	Rha	Rha		
1	102.3	102.4	102.3	102.3	102.1		
2	72.9	72.7	72.7	72.7	72.6		
3	73.0	72.9	72.9	72.9	72.7		
4	74.6	74.6	74.6	74.4	74.3		
5	69.8	69.8	69.7	69.8	69.5		
6	19.2	19.2	19.2	19.3	19.0		
28-O-		Glc	Glc	Glc	Glc	Glc	Glc
1		95.6	96.0	96.0	96.2	96.3	95.8
2		74.5	74.4	74.7	74.3	74.4	73.9
3		78.9	79.1	79.2	79.4	79.7	78.7
4		71.5	71.3	71.4	71.3	71.4	71.2
5		78.9	78.8	78.8	78.8	79.2	79.1
6		62.6	62.4	62.5	62.3	62.5	62.3

$\delta$  in ppm;  $J$  in Hz; <sup>a</sup> NMR spectra recorded at 100 MHz; <sup>b</sup> NMR spectra recorded at 150 MHz.



## 2.2. Anti-Inflammatory Activity

The anti-inflammatory activity of compounds 1–10 was evaluated by utilizing a LPS-stimulated RAW264.7 cell model. As presented in Figure 4, when compared with LPS stimulation in RAW264.7 cells, compounds 3, 5, and 6 exhibited inhibitory effects on the expression of iNOS protein, and the positive control drug dexamethasone (DEX) notably inhibited the expression of iNOS and COX-2 protein. The effects of DEX intervention suggested that the experimental procedure was adequate.

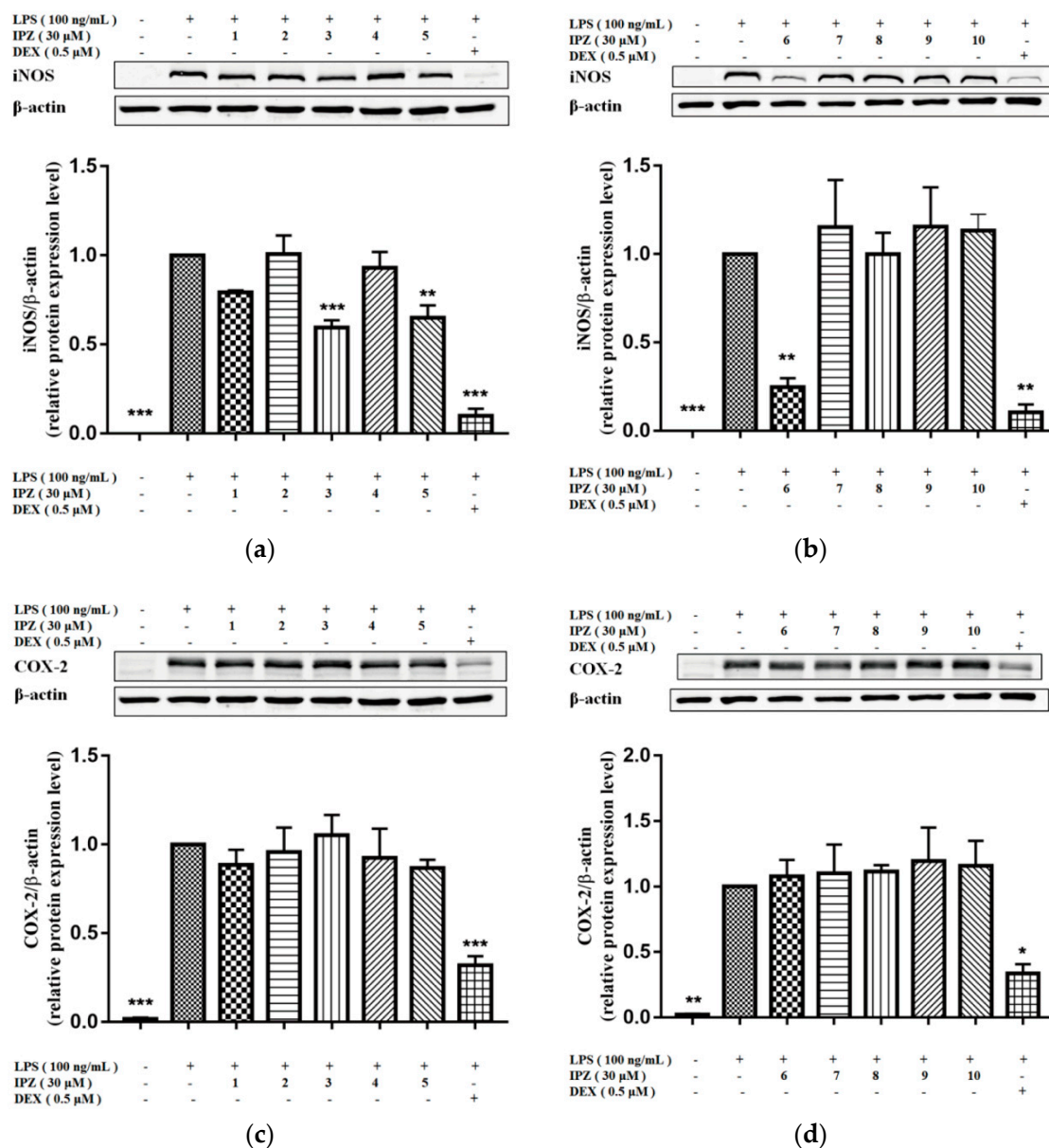


**Figure 4.** Effect of compounds 1–10 (IPZ 1–10) on inducible nitric oxide synthase (iNOS) and cyclooxygenase-2 (COX-2) protein expression in lipopolysaccharide (LPS)-stimulated RAW264.7 cells. RAW264.7 cells were seeded in 24-well plate and cultured overnight. Subsequently, compounds 1–10 and the positive control dexamethasone (DEX) were administered to RAW264.7 cells for 1 h, and LPS (100 ng/mL) was used to stimulate the cells for the final 18 h. Western blotting was performed to analyze protein expression of iNOS, COX-2, and the corresponding values were quantitated by Odyssey v3.0 software. The results are expressed as the mean  $\pm$  SEM,  $n = 3$ . \*  $p < 0.05$ , \*\*  $p < 0.01$ , \*\*\*  $p < 0.001$ , vs. LPS group.

### 3. Discussion

In summary, seven new triterpenoid saponins, named Pubescenosides E–K, together with three known ones, were isolated from the roots of *Ilex pubescens*. Elucidation of their structures was performed based on extensive spectroscopic analyses. The anti-inflammatory activity of the isolates toward lipopolysaccharide (LPS)-stimulated RAW264.7 macrophages was investigated. The results demonstrated that compounds 3, 5, and 6 inhibited iNOS protein expression in LPS-stimulated RAW264.7 cells with dexamethasone as a positive control. The findings revealed that compounds 3, 5, and 6 might have anti-inflammatory activity and might have potential value in anti-inflammatory treatments.

### 4. Materials and Methods

#### 4.1. General Experimental Procedures

A Jasco P-1020 digital polarimeter (Jasco, Tokyo, Japan) was used to measure the optical rotations at the sodium D line (589 nm). IR spectra were collected with a Jasco Fourier transform (FT)/IR-480 plus spectrophotometer (Jasco, Tokyo, Japan) for scanning the IR spectrum with KBr pellets. HRESIMS data were acquired on an Agilent 6540 Q-TOF mass spectrometer (Agilent Technologies, Palo Alto, CA, United States). The 1D and 2D NMR spectra were obtained using a Bruker AV-400 or a Bruker AV-600 spectrophotometer (Bruker, Faellanden, Switzerland), with tetramethylsilane in pyridine-*d*<sub>5</sub> as an internal standard. Semi-preparative HPLC was carried out with a LC-6AD pump and SPD-M20A detector on an Inertsil PREP-ODS (10  $\mu$ m, 20  $\times$  250 mm) column (GI Sciences Inc., Eindhoven, Netherlands). Silica gel (200–300 mesh, Qingdao Marine Chemical Plant, Qingdao, China), Sephadex LH-20 gel (25–100  $\mu$ m, GE Healthcare, Biosciences AB, Uppsala, Sweden), and reverse phase C18 (50  $\mu$ m, YMC, Kyoto, Japan) were used for column chromatography (CC). All reagents used were purchased from Tianjin Damao Chemical Company (Damao, Tianjin, China).

#### 4.2. Plant Material

The roots of *Ilex pubescens* were collected near Conghua City, Guangdong Province, China, in July 2012, and identified by Prof. Guangxiong Zhou of the College of Pharmacy, Jinan University. The voucher specimen (12071002) is stored in the International Institute for Translational Chinese Medicine, Guangzhou University of Traditional Chinese Medicine, Guangzhou, China.

#### 4.3. Extraction and Isolation

The powdered and dried roots of *I. pubescens* (40 kg) were extracted with 70% ethanol (2  $\times$  320 L) at 70 °C. The extract was evaporated under vacuum to obtain 2.2 kg of a dark brown residue. The residue was separated on a D101 macroporous resin column with different proportions of EtOH–H<sub>2</sub>O (0:10, 3:7, 6:4, and 9:1), which yielded four fractions (Frs. 1 to 4). Fr. 3 (500 g) was loaded on a silica gel CC with CHCl<sub>3</sub>–CH<sub>3</sub>OH (99:1–1:1) eluent to yield 12 fractions (Frs. A to L). Compound 1 (20 mg), was isolated from Fr. K by ODS CC using MeOH and H<sub>2</sub>O and further purified through RP-C<sub>18</sub> semi-preparative HPLC (MeOH–H<sub>2</sub>O 65:35; *t*<sub>R</sub>, 89.3 min). Fr. L (55 g) was separated into seven fractions (L<sub>1</sub>–L<sub>7</sub>) over silica gel CC with CH<sub>2</sub>Cl<sub>2</sub>–CH<sub>3</sub>OH (8:2–1:1) as the eluent. Fr. L<sub>2</sub> (15.8 g) was chromatographically separated on ODS CC with MeOH–H<sub>2</sub>O (40:60–100:0), followed by a Sephadex LH-20 column (MeOH), and purified by semi-preparative HPLC to achieve compound 6 (15 mg, MeOH–H<sub>2</sub>O 76.5:23.5; *t*<sub>R</sub>, 35.5 min). Fr. L<sub>3</sub> (17.5 g) was purified on ODS CC, eluting with MeOH–H<sub>2</sub>O (30:70–100:0) and further purified by semi-preparative HPLC to yield compound 2 (18 mg, MeOH–H<sub>2</sub>O 84:16; *t*<sub>R</sub>, 32 min); compound 3 (19 mg, MeOH–H<sub>2</sub>O 76:24; *t*<sub>R</sub>, 34.5 min); compound 5 (56 mg, MeOH–H<sub>2</sub>O 76:24; *t*<sub>R</sub>, 57 min); compound 7 (43 mg, CH<sub>3</sub>CN–H<sub>2</sub>O 22:78; *t*<sub>R</sub>, 32 min); compound 8 (32 mg, CH<sub>3</sub>CN–H<sub>2</sub>O 22:78; *t*<sub>R</sub>, 32 min); compound 9 (480 mg, MeOH–H<sub>2</sub>O 70:30; *t*<sub>R</sub>, 23 min); and compound 10 (10 mg, MeOH–H<sub>2</sub>O 76:24; *t*<sub>R</sub>, 20.5 min). Compound 4 (9.9 mg, MeOH–H<sub>2</sub>O, 62:28) was also obtained from Fr. L<sub>4</sub> through the chromatographic methods described above.

#### 4.3.1. Pubescenoside E (1)

White amorphous powder;  $[\alpha]_{\text{D}}^{25.8} +10.74$  (c 0.73 CH<sub>3</sub>OH); IR (KBr)  $\nu_{\text{max}}$ : 3426, 2938, 2874, 1703, 1644, 1357, 1041 cm<sup>-1</sup>; NMR spectroscopic data (pyridine-*d*<sub>5</sub>, 400/100 MHz), see Tables 1 and 2; HR-ESI-MS  $m/z$  955.4910 [M + COOH]<sup>-</sup> (calcd. for 955.4908).

#### 4.3.2. Pubescenoside F (2)

White amorphous powder;  $[\alpha]_{\text{D}}^{25.8} +3.52$  (c 0.97 CH<sub>3</sub>OH); IR (KBr)  $\nu_{\text{max}}$ : 3396, 2930, 2877, 1700, 1635, 1360, 1074 cm<sup>-1</sup>; NMR spectroscopic data (pyridine-*d*<sub>5</sub>, 600/150 MHz), see Tables 1 and 2; HR-ESI-MS  $m/z$  1071.5388 [M – H]<sup>-</sup> (calcd. for 1071.5381).

#### 4.3.3. Pubescenoside G (3)

White amorphous powder;  $[\alpha]_{\text{D}}^{25.8} +13.9$  (c 0.64 CH<sub>3</sub>OH); IR (KBr)  $\nu_{\text{max}}$ : 3408, 2930, 2870, 1738, 1646, 1384, 1077 cm<sup>-1</sup>; NMR spectroscopic data (pyridine-*d*<sub>5</sub>, 600/150 MHz), see Tables 1 and 2; HR-ESI-MS  $m/z$  1103.5642 [M + COOH]<sup>-</sup> (calcd. for 1103.5644).

#### 4.3.4. Pubescenoside H (4)

White amorphous powder;  $[\alpha]_{\text{D}}^{25.8} +14.6$  (c 0.63 CH<sub>3</sub>OH); IR (KBr)  $\nu_{\text{max}}$ : 3373, 2933, 2870, 1735, 1644, 1452, 1074 cm<sup>-1</sup>; NMR spectroscopic data (pyridine-*d*<sub>5</sub>, 600/150 MHz), see Tables 1 and 2; HR-ESI-MS  $m/z$  1073.5614 [M – H]<sup>-</sup> (calcd. for 1073.5538).

#### 4.3.5. Pubescenoside I (5)

White amorphous powder;  $[\alpha]_{\text{D}}^{25.8} -5.2$  (c 0.99 CH<sub>3</sub>OH); IR (KBr)  $\nu_{\text{max}}$ : 3396, 2930, 2877, 1729, 1641, 1360, 1077 cm<sup>-1</sup>; NMR spectroscopic data (pyridine-*d*<sub>5</sub>, 600/150 MHz), see Tables 1 and 2; HR-ESI-MS  $m/z$  1101.5488 [M + COOH]<sup>-</sup> (calcd. for 1101.5487).

#### 4.3.6. Pubescenoside J (6)

White amorphous powder;  $[\alpha]_{\text{D}}^{25.8} +10.2$  (c 0.53 CH<sub>3</sub>OH); IR (KBr)  $\nu_{\text{max}}$ : 3385, 2941, 2874, 1729, 1074 cm<sup>-1</sup>; NMR spectroscopic data (pyridine-*d*<sub>5</sub>, 600/150 MHz), see Tables 1 and 2; HR-ESI-MS  $m/z$  793.4462 [M + COOH]<sup>-</sup> (calcd. for 793.4380).

#### 4.3.7. Pubescenoside K (7)

White amorphous powder;  $[\alpha]_{\text{D}}^{25.8} +8.3$  (c 0.89 CH<sub>3</sub>OH); IR (KBr)  $\nu_{\text{max}}$ : 3458, 2938, 2880, 1735, 1646, 1230, 1065 cm<sup>-1</sup>; NMR spectroscopic data (pyridine-*d*<sub>5</sub>, 600/150 MHz), see Tables 1 and 2; HR-ESI-MS  $m/z$  845.4052 [M – H]<sup>-</sup> (calcd. for 845.3999).

#### 4.4. Acid Hydrolysis

Each solution of the seven new compounds (2 mg) was stirred in 2N HCl (5 mL) at 80 °C in a stoppered reaction vial for 5 h. The solution was evaporated to dryness under vacuum, and then the residue was compared with standard sugars by silica gel TLC. N-butanol-acetone-H<sub>2</sub>O (4:3:1) was chosen as the solvent system, and the spots were observed after spraying the plates with H<sub>2</sub>SO<sub>4</sub> and heating at 105 °C for 1 min. The *R<sub>f</sub>* values of xylose, glucose, and rhamnose via TLC, which were hydrolyzed from Pubescenoside E–K, were 0.47, 0.60, and 0.71, respectively. The residue was dissolved in pyridine, and 2 mg of L-cysteine methyl ester hydrochloride was added. The mixture was stirred at 60 °C for 2 h, 5 μL *O*-tolyl isothiocyanate was added, and the mixture was stirred at 60 °C for another 2 h. After cooling, the reaction mixture was analyzed by reversed phase HPLC (RP-C18 column, λ = 250 nm, acetonitrile–0.1% formic acid 25:75, flow rate, 1.0 mL/min). The retention time of D-xylose (*t<sub>R</sub>*, 18.4 min), D-glucose (*t<sub>R</sub>*, 15.8 min), and L-rhamnose (*t<sub>R</sub>*, 26.2 min) was determined by comparison with standards.

#### 4.5. Cell Culture and Western Blot

RAW264.7 cells were purchased from American Type Culture Collection (ATCC, Manassas, VA, USA) and cultured in Dulbecco's Modified Eagle's Medium containing 10% heat-inactivated fetal bovine serum, penicillin G (100 units/mL), streptomycin (100 mg/mL), and L-glutamine (2 mM) in a humidified incubator containing 5% CO<sub>2</sub> at 37 °C. Compounds 1–10 were completely dissolved in dimethyl sulfoxide to a final concentration of 30 mM, and the working concentration was 30 μM. RAW264.7 cells (8 × 10<sup>4</sup> cells/wells) were seeded in 24-well plates for 24 h, pretreated with compounds 1–10 or dexamethasone for 1 h, and then stimulated with LPS (100 ng/mL) for another 18 h. Dexamethasone at a concentration of 0.5 μM was selected as a positive control for inhibition of iNOS and COX-2 expression. LPS-stimulated cells without any intervention were used as the model control, and cells cultured in DMEM medium were used as the normal control. The Western blot methods were based on our previous research [19].

**Supplementary Materials:** The IR, HRESIMS, and 1D and 2D NMR spectra of the new compounds are available in the supplementary materials.

**Author Contributions:** Z.L., H.Z., P.W., and G.L. conceived and designed the experiments; X.Q., L.M., and M.J. isolated the compounds; X.Q. elucidated the structures; Y.Y. carried out the biological assay and helped with the preparation of the manuscript; X.Q. wrote the paper; and P.W. managed the research project. All authors read and approved the final manuscript.

**Acknowledgments:** This research was funded by the grants of National Natural Science Foundation of China [grant number 81503224], Science and Technology Project of Guangdong Province [grant number 2016A050502052], Department of education of Guangdong Province [grant number 2016KZDXM031 and 2016KQNCX026], and Science and Technology Project of Guangzhou City [grant number 201707010467].

**Conflicts of Interest:** The authors declare no conflict of interest.

#### References

1. Lin, L.P.; Wei, Q.U.; Liang, J.Y. Chemical constituents from the stems of *Ilex pubescens* var. *glabra*. *Chin. J. Nat. Med.* **2011**, *9*, 176–179.
2. Han, Y.N.; Bail, S.K.; Kim, T.H.; Han, B.H. New triterpenoid saponins from *Ilex pubescens*. *Arch. Pharm. Res.* **1987**, *10*, 132–141. [[CrossRef](#)]
3. Jiangsu New Medical College. *Directory of Chinese Material Medica*, 1st ed.; Shanghai Scientific and Technological Press: Shanghai, China, 1997; p. 441.
4. Zhou, Y.; Chai, X.Y.; Zeng, K.W.; Zhang, J.Y.; Li, N.; Jiang, Y.; Tu, P.F. Ilex pubescens C–M, eleven new triterpene saponins from the roots of *Ilex pubescens*. *Planta Med.* **2013**, *79*, 70–77. [[PubMed](#)]
5. Xu, Z.R.; Chai, X.Y.; Bai, C.C.; Ren, H.Y.; Lu, Y.N.; Shi, H.M.; Tu, P.F. Xylocosides A–G, phenolic glucosides from the stems of *xylosma controversum*. *Helv. Chim. Acta* **2010**, *91*, 1346–1354. [[CrossRef](#)]
6. Gohari, A.R.; Saeidnia, S.; Bayati-Moghadam, M.; Gh, A. Lignans and neolignans from *Stelleropsis antoninae*. *DRAU* **2011**, *19*, 74–79.
7. Jiang, Z.H.; Wang, J.R.; Li, M.; Liu, Z.Q.; Chau, K.Y.; Zhao, C.; Liu, L. Hemiterpene glucosides with anti-platelet aggregation activities from *Ilex pubescens*. *J. Nat. Prod.* **2008**, *68*, 397–399. [[CrossRef](#)] [[PubMed](#)]
8. Cao, L.H.; Zheng, Y.; Xin, W.Y.; Xu, K.; Miao, M.S. Study on intervention action of total flavonoids from *Ilex pubescens* Radix on animal models of cerebral ischemic tolerance with blood stasis. *China J. Chin. Mater. Med.* **2016**, *41*, 3419–3424.
9. Wang, J.R.; Zhou, H.; Jiang, Z.H.; Liu, L. Two new triterpene saponins from the anti-inflammatory saponin fraction of *Ilex pubescens* root. *Chem. Biodivers.* **2008**, *5*, 1369–1376. [[CrossRef](#)] [[PubMed](#)]
10. Fabio, G.D.; Romanucci, V.; Marco, A.D.; Zarrelli, A. Triterpenoids from *Gymnema sylvestre* and their pharmacological activities. *Molecules* **2014**, *19*, 10956–10981. [[CrossRef](#)] [[PubMed](#)]
11. Fabio, G.D.; Romanucci, V.; Zarrelli, M.; Giordano, M.; Zarrelli, A. C-4 gem-dimethylated oleanes of *Gymnema sylvestre* and their pharmacological activities. *Molecules* **2013**, *18*, 14892–14919. [[CrossRef](#)] [[PubMed](#)]
12. Armo, Z.; Marina, D.G.; Afef, L.; Rabiaa, H.; Lucio, P. New triterpenes from *Gymnema sylvestre*. *Helv. Chim. Acta* **2013**, *96*, 1036–1045.

13. Han, Y.N.; Song, J.I.; Rhee, I.K. Anticoagulant activity of ilexoside D, a triterpenoid saponin from *Ilex pubescens*. *Arch. Pharm. Res.* **1993**, *16*, 209–212. [[CrossRef](#)]
14. Han, Y.N.; Baik, S.K.; Kim, T.H.; Han, B.H. Antithrombotic activities of saponins from *Ilex pubescens*. *Arch. Pharm. Res.* **1987**, *10*, 115–120. [[CrossRef](#)]
15. Ryu, H.W.; Su, U.L.; Lee, S.; Song, H.H.; Son, T.H.; Kim, Y.U.; Yuk, H.J.; Ro, H.; Lee, C.K.; Hong, S.T. 3-Methoxy-catalposide inhibits inflammatory effects in lipopolysaccharide-stimulated RAW264.7 macrophages. *Cytokine* **2017**, *91*, 57–64. [[CrossRef](#)] [[PubMed](#)]
16. Dong, J.S.; Li, J.J.; Cui, L.Y.; Wang, Y.F.; Lin, J.Q.; Qu, Y.; Wang, H. Cortisol modulates inflammatory responses in LPS-stimulated RAW264.7 cells via the NF- $\kappa$ B and MAPK pathways. *BMC Vet. Res.* **2018**, *14*, 30–40. [[CrossRef](#)] [[PubMed](#)]
17. Zhao, H.; Wang, Q.L.; Hou, S.B.; Chen, G. Chemical constituents from the rhizomes of *Polygonatum sibiricum* Red. and anti-inflammatory activity in RAW264.7 macrophage cells. *Nat. Prod. Res.* **2018**, *8*, 1–4. [[CrossRef](#)] [[PubMed](#)]
18. Choy, C.S.; Hu, C.M.; Chiu, W.T.; Lam, C.S.; Ting, Y.; Tsai, S.H.; Wang, T.C. Suppression of lipopolysaccharide-induced of inducible nitric oxide synthase and cyclooxygenase-2 by Sanguis Draconis, a dragon's blood resin, in RAW 264.7 cells. *J. Ethnopharmacol.* **2008**, *115*, 455–462. [[CrossRef](#)] [[PubMed](#)]
19. Wu, P.; Gao, H.; Liu, J.X.; Liu, L.; Zhou, H.; Liu, Z.Q. Triterpenoid saponins with anti-inflammatory activities from *Ilex pubescens* roots. *Phytochemistry* **2017**, *134*, 122–132. [[CrossRef](#)] [[PubMed](#)]
20. Kakuno, T.; Yoshikawa, K.; Arihara, S. Ilexosides A, B, C and D, anti-allergic 18,19-seco-ursane glycosides from fruit of *Ilex crenata*. *Tetrahedron Lett.* **1991**, *32*, 3535–3538. [[CrossRef](#)]
21. Abdel-Sattar, E. Saponin glycosides from *Osteospermum vaillantii*. *Pharm. Biol.* **2001**, *39*, 440–444. [[CrossRef](#)]

**Sample Availability:** Samples of the compounds 1–10 are available from the authors.



© 2018 by the authors. Licensee MDPI, Basel, Switzerland. This article is an open access article distributed under the terms and conditions of the Creative Commons Attribution (CC BY) license (<http://creativecommons.org/licenses/by/4.0/>).